



W&M ScholarWorks

Arts & Sciences Articles

Arts and Sciences

2014

Strangeness Suppression of $q(\bar{q})$ Creation Observed in Exclusive Reactions

A. El Alaoui

C. I. Moody

M. H. Wood

K. A. Griffioen

College of William and Mary

Follow this and additional works at: <https://scholarworks.wm.edu/aspubs>

Recommended Citation

Park, K & D. Mestayer, M. (2014). Strangeness Suppression in $q\bar{q}$ Creation Observed in Exclusive Reactions. *Physical Review Letters*. 113. 10.1103/PhysRevLett.113.152004.

This Article is brought to you for free and open access by the Arts and Sciences at W&M ScholarWorks. It has been accepted for inclusion in Arts & Sciences Articles by an authorized administrator of W&M ScholarWorks. For more information, please contact scholarworks@wm.edu.

Strangeness Suppression in $q\bar{q}$ Creation Observed in Exclusive Reactions

M.D. Mestayer,³² K. Park,^{32,*} K.P. Adhikari,²⁶ M. Aghasyan,¹⁵ S. Anefalos Pereira,¹⁵ J. Ball,⁶ M. Battaglieri,¹⁶ V. Batourine,³² I. Bedlinskiy,¹⁹ A.S. Biselli,^{9,4} S. Boiarinov,³² W.J. Briscoe,¹² W.K. Brooks,^{33,32} V.D. Burkert,³² D.S. Carman,³² A. Celentano,¹⁶ S. Chandavar,²⁵ G. Charles,¹⁸ L. Colaneri,^{29,17} P.L. Cole,^{13,32} M. Contalbrigo,¹⁴ O. Cortes,¹³ V. Crede,¹¹ A. D'Angelo,^{17,29} N. Dashyan,³⁸ R. De Vita,¹⁶ A. Deur,³² C. Djalali,³¹ D. Doughty,^{7,32} R. Dupre,¹⁸ A. El Alaoui,^{1,†} L. El Fassi,²⁶ L. Elouadrhiri,³² P. Eugenio,¹¹ G. Fedotov,^{31,30} J.A. Fleming,³⁴ T.A. Forest,¹³ B. Garillon,¹⁸ M. Garçon,⁶ Y. Ghandilyan,³⁸ G.P. Gilfoyle,²⁸ K.L. Giovanetti,²⁰ F.X. Girod,³² J.T. Goetz,²⁵ E. Golovatch,³⁰ R.W. Gothe,³¹ K.A. Griffioen,³⁷ B. Guegan,¹⁸ M. Guidal,¹⁸ H. Hakobyan,^{33,38} C. Hanretty,^{36,‡} M. Hattawy,¹⁸ M. Holtrop,²³ S.M. Hughes,³⁴ Y. Ilieva,^{31,12} D.G. Ireland,³⁵ H. Jiang,³¹ H.S. Jo,¹⁸ K. Joo,⁸ D. Keller,³⁶ M. Khandaker,^{13,24} A. Kim,^{21,§} W. Kim,²¹ S. Koirala,²⁶ V. Kubarovskiy,^{32,27} S.V. Kuleshov,^{33,19} P. Lenisa,¹⁴ W.I. Levine,⁴ K. Livingston,³⁵ H.Y. Lu,³¹ I. J. D. MacGregor,³⁵ M. Mayer,²⁶ B. McKinnon,³⁵ C.A. Meyer,⁴ M. Mirazita,¹⁵ V. Mokeev,^{32,30} R.A. Montgomery,^{15,¶} C.I. Moody,¹ H. Moutarde,⁶ A. Movsisyanyan,¹⁴ C. Munoz Camacho,¹⁸ P. Nadel-Turonski,³² S. Niccolai,^{18,12} G. Niculescu,^{20,25} I. Niculescu,²⁰ M. Osipenko,¹⁶ A.I. Ostrovidov,¹¹ L.L. Pappalardo,¹⁴ R. Paremuzyan,^{38,**} P. Peng,³⁶ W. Phelps,¹⁰ S. Pisano,¹⁵ O. Pogorelko,¹⁹ S. Pozdniakov,¹⁹ J.W. Price,^{27,3} D. Protopopescu,³⁵ A.J.R. Puckett,⁸ B.A. Raue,^{10,32} D. Rimal,¹⁰ M. Ripani,¹⁶ A. Rizzo,¹⁷ P. Roy,¹¹ F. Sabatié,⁶ M.S. Saini,¹¹ D. Schott,¹² R.A. Schumacher,⁴ A. Simonyan,³⁸ D. Sokhan,³⁵ S. Strauch,^{31,12} V. Sytnik,³³ W. Tang,²⁵ Ye Tian,³¹ M. Ungaro,^{32,27} B. Vernarsky,⁴ A.V. Vlassov,¹⁹ H. Voskanyan,³⁸ E. Voutier,²² N.K. Walford,⁵ D.P. Watts,³⁴ X. Wei,³² L.B. Weinstein,²⁶ M.H. Wood,^{2,31} N. Zachariou,³¹ J. Zhang,³² Z.W. Zhao,³⁶ and I. Zonta¹⁷

(The CLAS Collaboration)

¹Argonne National Laboratory, Argonne, Illinois 60439, USA

²Canisius College, Buffalo, New York, USA

³California State University, Dominguez Hills, Carson, California 90747, USA

⁴Carnegie Mellon University, Pittsburgh, Pennsylvania 15213, USA

⁵Catholic University of America, Washington, D.C. 20064, USA

⁶CEA, Centre de Saclay, Irfu/Service de Physique Nucléaire, 91191 Gif-sur-Yvette, France

⁷Christopher Newport University, Newport News, Virginia 23606, USA

⁸University of Connecticut, Storrs, Connecticut 06269, USA

⁹Fairfield University, Fairfield Connecticut 06824, USA

¹⁰Florida International University, Miami, Florida 33199, USA

¹¹Florida State University, Tallahassee, Florida 32306, USA

¹²The George Washington University, Washington, D.C. 20052, USA

¹³Idaho State University, Pocatello, Idaho 83209, USA

¹⁴INFN, Sezione di Ferrara, 44100 Ferrara, Italy

¹⁵INFN, Laboratori Nazionali di Frascati, 00044 Frascati, Italy

¹⁶INFN, Sezione di Genova, 16146 Genova, Italy

¹⁷INFN, Sezione di Roma Tor Vergata, 00133 Rome, Italy

¹⁸Institut de Physique Nucléaire ORSAY, Orsay, France

¹⁹Institute of Theoretical and Experimental Physics, Moscow, 117259, Russia

²⁰James Madison University, Harrisonburg, Virginia 22807, USA

²¹Kyungpook National University, Daegu 702-701, Republic of Korea

²²LPSC, Université Grenoble-Alpes, CNRS/IN2P3, Grenoble, France

²³University of New Hampshire, Durham, New Hampshire 03824-3568, USA

²⁴Norfolk State University, Norfolk, Virginia 23504, USA

²⁵Ohio University, Athens, Ohio 45701, USA

²⁶Old Dominion University, Norfolk, Virginia 23529, USA

²⁷Rensselaer Polytechnic Institute, Troy, New York 12180-3590, USA

²⁸University of Richmond, Richmond, Virginia 23173, USA

²⁹Università di Roma Tor Vergata, 00133 Rome Italy

³⁰Skobeltsyn Institute of Nuclear Physics, Lomonosov Moscow State University, 119234 Moscow, Russia

³¹University of South Carolina, Columbia, South Carolina 29208, USA

³²Thomas Jefferson National Accelerator Facility, Newport News, Virginia 23606, USA

³³Universidad Técnica Federico Santa María, Casilla 110-V Valparaíso, Chile

³⁴Edinburgh University, Edinburgh EH9 3JZ, United Kingdom

³⁵University of Glasgow, Glasgow G12 8QQ, United Kingdom

³⁶University of Virginia, Charlottesville, Virginia 22901, USA

³⁷College of William and Mary, Williamsburg, Virginia 23187-8795, USA

³⁸Yerevan Physics Institute, 375036 Yerevan, Armenia

We measured the ratios of electroproduction cross-sections from a proton target for three exclusive meson-baryon final states: ΛK^+ , $p\pi^0$, and $n\pi^+$, with the CLAS detector at Jefferson Lab. Using a simple model of quark hadronization we extract $q\bar{q}$ creation probabilities for the first time in exclusive two-body production, in which only a single $q\bar{q}$ pair is created. We observe a sizable suppression of strange quark-antiquark pairs compared to non-strange pairs, similar to that seen in high-energy production.

PACS numbers: 13.60.Le,13.60.Rj,13.87.Fh,14.65.Bt

At high energies the production of hadrons is well described by a model in which the color “flux-tube” is “broken” by a series of $q\bar{q}$ pair creation events followed by a regrouping of the quarks and anti-quarks into color singlet hadrons. The modeling of the strong force as a color flux tube explained the linear binding potential of heavy $q\bar{q}$ “quarkonia” states, while quark-pair creation models [1] developed in the 1970’s accounted for hadronic production and the non-observance of free quarks.

The “Lund Model” [2] was formulated in the 1980’s to quantify the fragmentation of very high-momentum quarks into “jets” of observed hadrons. The $q\bar{q}$ pair creation process is modeled as tunneling in a linear potential, resulting in a probability proportional to the exponential of the quark mass squared divided by the flux-tube tension of ≈ 1 GeV/fm. Calculations with plausible quark masses indicated that $s\bar{s}$ production is reduced by a factor of about one-third relative to that for $u\bar{u}$ or $d\bar{d}$. This reduction factor is known as the “strangeness suppression factor”, and is empirically adjusted to approximate the observed production rates of hadrons.

Strangeness suppression has been studied by various hadron-production experiments [3] resulting in a successful extension of the Lund Model into, among others, the JETSET and PYTHIA event generators [4] which reproduce observed hadronic production rates in high energy reactions. Typically, a strangeness suppression factor, $\lambda_s \approx 0.3$ describes the data well in e^+e^- collisions up to

center-of-mass energies of the Z boson mass [5] and in high-energy deep-inelastic electron proton scattering [6].

Although $q\bar{q}$ creation is the “kernel” of the process which transforms quarks into observable hadrons, it is not well-understood. We designed our study to extract the flavor-dependence of $q\bar{q}$ creation in a new kinematic region: the two-body exclusive limit in which a single $q\bar{q}$ pair is created, there are no decay chains to model and for which we can do an explicit phase-space correction.

In pseudoscalar-meson electroproduction, a beam of electrons is incident upon a proton target, producing a final state consisting of the scattered electron and the outgoing baryon and pseudo-scalar meson. After integrating over the azimuthal angle of the scattered electron, the cross section can be expressed in terms of the variables Q^2 , W , θ_m^* , and ϕ , where $q^2 = -Q^2$ is the squared four-momentum of the virtual photon, W is the total hadronic energy in the center-of-mass frame, θ_m^* is the meson angle in the γ^*p center-of-mass system and ϕ is the azimuthal angle of the reaction plane with respect to the electron scattering plane:

The differential cross-section can be expressed as:

$$\frac{d\sigma}{dQ^2 dW d\Omega_m^*} = \Gamma_v \left(\sigma_T + \epsilon \sigma_L + \epsilon \sigma_{TT} \cos 2\phi + \sqrt{\epsilon(\epsilon+1)} \sigma_{LT} \cos \phi \right), \quad (1)$$

where Γ_v is the flux of virtual photons, ϵ is the polarization parameter, and the four structure functions, σ_T , σ_L , σ_{TT} and σ_{LT} are the transverse and longitudinal response functions and the two interference terms, respectively. This formalism is explained in more detail in a previous CLAS collaboration paper [7].

Our study was part of a larger program to measure electroproduction of hadrons from a proton target. The electron beam energy was 5.499 GeV, with a typical intensity of 7 nA, incident on a 5-cm liquid hydrogen target. The signal from the scattered electron provided the data-acquisition trigger. The data-taking period lasted for 42 days and resulted in the collection of ~ 4.3 billion events. After event reconstruction, ~ 650 million events

*Current address:Old Dominion University, Norfolk, Virginia 23529, USA

†Current address:Universidad Técnica Federico Santa María, Casilla 110-V Valparaíso, Chile

‡Current address:Thomas Jefferson National Accelerator Facility, Newport News, Virginia 23606, USA

§Current address:University of Connecticut, Storrs, Connecticut 06269, USA

¶Current address:University of Glasgow, Glasgow G12 8QQ, United Kingdom

**Current address:Institut de Physique Nucléaire ORSAY, Orsay, France

remained with at least one good electron candidate.

The scattered electron and associated hadrons were measured in the CLAS detector, a large-acceptance magnetic spectrometer [8] based on a six-coil toroidal magnet with drift chambers providing charged particle tracking, followed by a Cherenkov detector for electron identification, and scintillators and an electromagnetic calorimeter for particle identification by time-of-flight and energy deposition, respectively.

The electron was identified by matching a negatively-charged track in the drift chambers with signals in the Cherenkov counter and in the electromagnetic calorimeter. The identity of the positively-charged particle candidate was determined by combining the flight time from the time-of-flight counters with the momentum and track length from the drift chamber track to calculate the particle's velocity (β) and mass.

We analyzed events with a final state consisting of the scattered electron plus one positively charged particle (a K^+ , π^+ or proton). We measured the four-momenta of the scattered electron and charged hadron, and determined by missing-mass that the undetected neutral particle was a Λ , a neutron or a π^0 , respectively.

The scattered electron's and charged hadron's four momenta were used to calculate the independent kinematic variables: Q^2 , W , $\cos\theta_m^*$ and ϕ . Our kinematic coverages are $W = 1.65 - 2.55$ GeV, $Q^2 = 1.6 - 4.6$ GeV² and the full range of $\cos\theta_m^*$ and ϕ . We defined 720 bins in this four-dimensional space (see Table I).

Quantity	No. Bin	Bin Limits
W (GeV)	6	1.65, 1.75, 1.85, 1.95, 2.05, 2.25, 2.55
Q^2 (GeV ²)	2	1.6, 2.6, 4.6
$\cos\theta_m^*$	5	-1.0, -0.6, -0.2, 0.2, 0.6, 1.0
ϕ (deg)	12	-180., -150., ... 150., 180.

TABLE I: Kinematic binning used in this analysis.

For each event, the missing-mass recoiling from the scattered electron and identified hadron was calculated and, by accumulating over all events, a missing-mass distribution was formed for each four-dimensional kinematic bin. For the $p\pi^0$ final state, an additional series of cuts was employed to remove radiative elastic-scattering events before our fits and mass cuts were applied. We then fit each missing-mass distribution to a function consisting of a Gaussian peak for the signal and a smooth polynomial for the background. We subtracted the background portion of the fit and counted the number of events within a fixed missing-mass range to obtain the raw yield, using the fit values for determination of the statistical uncertainty of the yield.

Corrections for finite acceptance and inefficiencies in

Procedure	Systematic Uncertainty		
	$n\pi^+$	$p\pi^0$	ΛK^+
Raw Yield Determination	7%	17%	12%
Hadron PID cuts	3%	10%	11%
Missing-mass cuts	3.5%	10.5%	2.5%
Background subtraction	5%	6%	0.3%
Efficiency Correction	6%	5%	5%
Event generator dependence	1%	1%	0.7%
Fiducial cuts	2.5%	0.5%	0.2%
Trigger/Tracking eff.	5%	5%	5%
Phase Space Correction	1.0%	0.4%	0.1%
Total Uncertainty	9%	18%	13%

TABLE II: Sources and estimates of systematic uncertainties of the acceptance-corrected yields.

track reconstruction, particle identification and missing-mass cuts were made. A Monte Carlo simulation, tuned to match the momentum resolution of the detector, accounted for run-dependent inefficiencies due to malfunctioning sub-system components.

The acceptance-corrected yields were further corrected by a two-body phase-space factor [9],

$$\Delta\rho_2 = |\mathbf{K}_1|/(16\pi^2 W), \quad (2)$$

where $|\mathbf{K}_1|$, the momentum in the center-of-mass frame, and W are evaluated at bin center. We did not correct our data for radiative effects because explicit calculations showed that the radiative correction factors for the ΛK^+ and $n\pi^+$ channels agreed within $\pm 10\%$ for all bins [10], which is smaller than the systematic uncertainty of the ratio, and showed no discernible kinematic dependence. Some corrected yields for the $p\pi^0$ channel were rejected for further analysis if the acceptance for the bin in question was lower than 2%.

The major sources and sizes of systematic uncertainties in the determination of the yields are summarized in Table II, grouped by category. Overall, we assign a systematic uncertainty of 9%, 18% or 13% to the $n\pi^+$, $p\pi^0$ or ΛK^+ corrected yields, respectively.

We then fit the ϕ distributions of the corrected yields in each bin of Q^2 , W and $\cos\theta_m^*$ to the form $A + B \cos 2\phi + C \cos \phi$. Some fits were rejected in the case of the $p\pi^0$ channel if there were fewer than 9 ϕ data points (of a nominal 12) surviving the minimum acceptance cut. This procedure resulted in 60 independent fitted values of the (A) terms for the ΛK^+ and $n\pi^+$ channels, but only 48 for the $p\pi^0$ channel. We divided the (A) terms for the different channels to form the cross-section ratios [11].

Figure 1 shows the three ratios of corrected yields plotted versus $\cos\theta_m^*$ with the different symbols representing different W bins. The two columns show the $\langle Q^2 \rangle = 1.9$ GeV² bin (left) and the $\langle Q^2 \rangle = 3.2$ GeV² bin (right).

The shaded band is centered on the statistical average for each $\cos\theta_m^*$ bin with half-width equal to the systematic uncertainty on the ratio. Note that the three ratios are approximately the same for the two Q^2 bins while there is a noticeable fall-off of the $\Lambda K^+/n\pi^+$ and $p\pi^0/n\pi^+$ ratios with $\cos\theta_m^*$. Figure 2 shows the same ratios as in Figure 1, but plotted versus W . Again the two columns are for the two bins in Q^2 . One can see that the ratios are approximately independent of W .

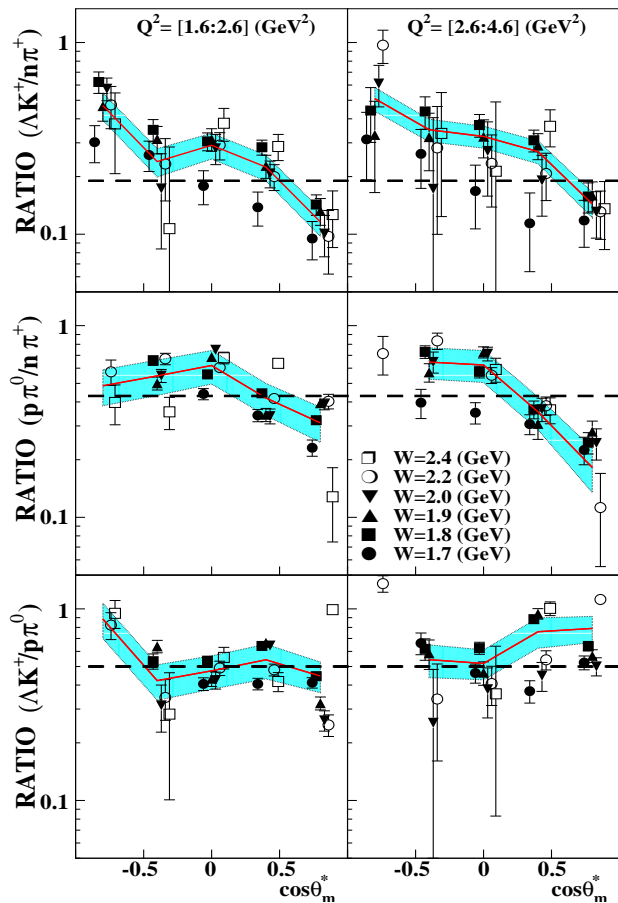


FIG. 1: (Color online) Ratio of the three exclusive cross-sections, ΛK^+ to $n\pi^+$ (top), $p\pi^0$ to $n\pi^+$ (middle) and ΛK^+ to $p\pi^0$ (bottom), for bins of $\langle Q^2 \rangle = 1.9 \text{ GeV}^2$ (left) and $\langle Q^2 \rangle = 3.2 \text{ GeV}^2$ (right), plotted versus $\cos\theta_m^*$ with different bins in W shown as different symbols. The systematic uncertainty is indicated by the shaded band, centered on the solid (red) line which connects the statistically-weighted average for each bin. The flat dashed line represents the overall statistical average for each ratio. The data points are plotted slightly offset for clarity.

For purposes of comparing with the single value of λ_s used to characterize the ratio of strange to non-strange hadronic production at high energy, we performed a

weighted average over all bins for each ratio of final states, indicated by the flat dashed line. We obtain the following average values for the ratios: $\langle \Lambda K^+/n\pi^+ \rangle = 0.19 \pm 0.01 \pm 0.03$, $\langle p\pi^0/n\pi^+ \rangle = 0.43 \pm 0.01 \pm 0.09$, and $\langle \Lambda K^+/p\pi^0 \rangle = 0.50 \pm 0.02 \pm 0.12$; the first uncertainty is statistical and the second systematic.

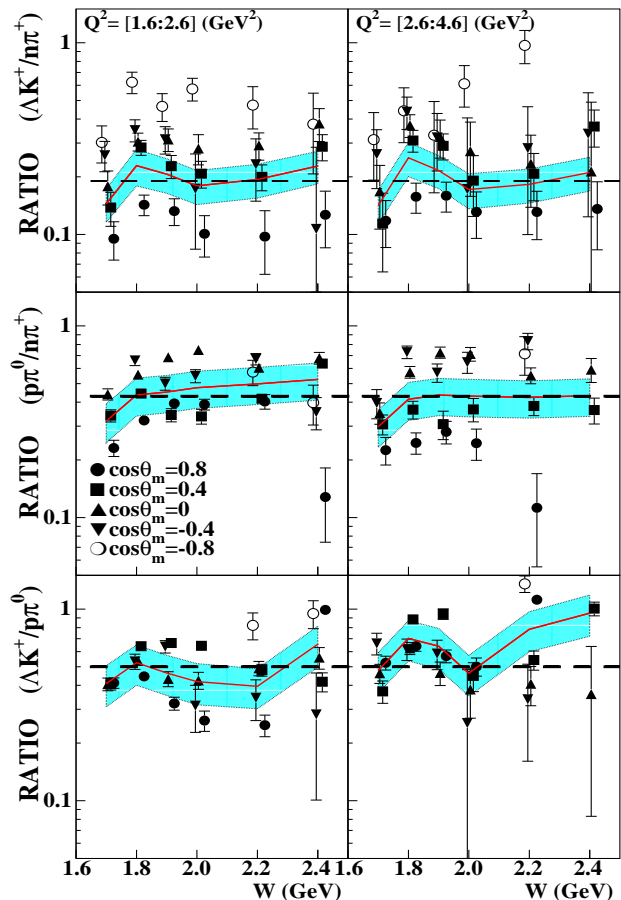


FIG. 2: (Color online) Ratio of the three exclusive cross-sections, displayed as in Figure 1, but plotted versus W with different bins of $\cos\theta_m^*$ shown as different symbols.

We extracted the ratio of $q\bar{q}$ creation probabilities from these measured hadronic ratios using a simple factorization model in which a quark is knocked out of the proton followed by a single $q\bar{q}$ creation and appearance of the lightest baryon and pseudo-scalar meson consistent with the quark flavor. We ignored other processes such as vector-meson coupling to the virtual photon or t -channel exchange, which might be responsible for the $\cos\theta_m^*$ dependence of our data. Nevertheless, we hope that the results from our simplified modelling are useful for comparison with strangeness suppression results from semi-inclusive production experiments analysed under similar

factorization assumptions. We note similarities of our model with that used by M. M. Kaskulov *et al.* [12] in fitting other data from Jefferson Lab on electroproduction of $n\pi^+$ from the proton.

In our model, events are initiated by virtual photon absorption by a valence u -quark or d -quark in the ratio of the sums of squares of the quark charges (8:1). This is followed by a single $q\bar{q}$ produced with probability $\mathbf{P}(q\bar{q})$, resulting in a $q\bar{q}$ state recoiling from a qqq state. Finally, the $q\bar{q}$ state hadronizes into the lowest energy meson state and the qqq state hadronizes into the lowest energy baryon state, in both cases with unit probability, resulting in three possible final states: $n\pi^+$, $p\pi^0$ or ΛK^+ . Note also that we take into account that the π^0 is a 50 : 50 mixture of $u\bar{u}$ and $d\bar{d}$.

Following this simple arithmetic, the hadronic production rates (\mathfrak{R}) can be written in terms of the $q\bar{q}$ probabilities ($\mathbf{P}(q\bar{q})$) as such:

$$\mathfrak{R}(\Lambda K^+) \propto 8 \cdot \mathbf{P}(s\bar{s}), \quad \mathfrak{R}(n\pi^+) \propto 8 \cdot \mathbf{P}(d\bar{d}), \text{ and}$$

$$\mathfrak{R}(p\pi^0) \propto 1/2 \cdot (8 \cdot \mathbf{P}(u\bar{u}) + 1 \cdot \mathbf{P}(d\bar{d})).$$

We use the $\langle \Lambda K^+ / n\pi^+ \rangle$ ratio to solve for $s\bar{s}/d\bar{d}$ and the $\langle p\pi^0 / n\pi^+ \rangle$ ratio to solve for $u\bar{u}/d\bar{d}$:

$$s\bar{s}/d\bar{d} = \langle \Lambda K^+ / n\pi^+ \rangle = 0.19 \pm 0.01 \pm 0.03 ,$$

$$u\bar{u}/d\bar{d} = 2 (\langle p\pi^0 / n\pi^+ \rangle - 1/16) = 0.74 \pm 0.02 \pm 0.18$$

Finally, we use the $\langle \Lambda K^+ / p\pi^0 \rangle$ ratio to determine an independent measure of the $s\bar{s}/d\bar{d}$ ratio. We obtain $s\bar{s}/d\bar{d} = 1/2 (u\bar{u}/d\bar{d} + 1/8)\langle \Lambda K^+ / p\pi^0 \rangle$, yielding

$$s\bar{s}/d\bar{d} = 0.28 \pm 0.01 \pm 0.07 \quad \text{assuming } u\bar{u}/d\bar{d} = 1.0, \text{ or}$$

$$s\bar{s}/d\bar{d} = 0.22 \pm 0.01 \pm 0.07 \quad \text{assuming } u\bar{u}/d\bar{d} = 0.74$$

(as measured).

The systematic uncertainty on a $q\bar{q}$ ratio is simply that of the particle production ratio from which it is derived. We do not include factors due to the angular dependence of the ratios, nor do we attempt to quantify the systematic uncertainty of our hadronization model. Table III summarizes the results of this extraction.

Ratio	$s\bar{s}/d\bar{d}$	$u\bar{u}/d\bar{d}$
$\Lambda K^+ / n\pi^+$	0.19 ± 0.03	–
$\Lambda K^+ / p\pi^0$ “ a ”	0.22 ± 0.07	–
$\Lambda K^+ / p\pi^0$ “ b ”	0.28 ± 0.07	–
$p\pi^0 / n\pi^+$	–	0.74 ± 0.18

TABLE III: Values of ratio of $s\bar{s}$ to $d\bar{d}$ and $u\bar{u}$ to $d\bar{d}$ shown according to the experimental ratios from which they are derived. The “**a**” and “**b**” cases for the $\Lambda K^+ / p\pi^0$ data-set refer to the values of $u\bar{u}/d\bar{d}$ used in the extraction of the $s\bar{s}/d\bar{d}$ ratio: 0.74 for the “**a**” case and 1.0 for the “**b**” case. The uncertainties are the systematic uncertainties.

We point out that our result of 0.74 ± 0.18 for the $u\bar{u}/d\bar{d}$ ratio is different from the value of unity expected from isospin invariance arguments, as assumed, for example, in high-energy hadronization models. However, we note that our hadron-production environment is explicitly not isospin invariant because the target is a proton, with two valence u -quarks and one valence d -quark. We speculate that the isospin-dependence of our result for the $u\bar{u}/d\bar{d}$ ratio is related to the difference between the intrinsic \bar{u} and \bar{d} content of the proton as measured in Drell-Yan[13] and semi-inclusive DIS experiments[14]. Although intriguing, unfortunately our measurement is not significantly different from unity, especially when model uncertainties are included.

To summarize, our results show a sizable suppression of the ΛK^+ channel relative to the $n\pi^+$ and $p\pi^0$ channels from which we use a simple factorization model to estimate a strangeness suppression factor ($s\bar{s}/d\bar{d}$) of 0.19 ± 0.03 , 0.22 ± 0.07 or 0.28 ± 0.07 , depending on which data ratios we use and what we assume for the $u\bar{u}/d\bar{d}$ ratio. Interestingly, these values are similar to measurements of flavor suppression at high energies [3], [5], [6].

These determinations of the flavor dependence of $q\bar{q}$ creation are the first in the low-energy exclusive limit where the connection between the observed hadronic ratios and $q\bar{q}$ production probabilities is simple because only a single $q\bar{q}$ pair is created. However, further development of exclusive reaction theory is needed to reduce the model dependence in the extraction of the $q\bar{q}$ creation probabilities from our data. We conclude by noting that understanding $q\bar{q}$ production dynamics is an important part of understanding color confinement in QCD and the fact that our values for strangeness suppression agree well with measurements done at much higher energy argues strongly for the universal nature of these dynamics.

We thank the staff of the Accelerator and Physics Divisions at Jefferson Lab for making the experiment possible. We also thank C. Weiss for many informative discussions. This work was supported in part by the US Department of Energy, the National Science Foundation, the Italian Istituto Nazionale di Fisica Nucleare, the French American Cultural Exchange (FACE) and Partner University Funds (PUF) programs, the French Centre National de la Recherche Scientifique, the French Commissariat à l’Energie Atomique, the United Kingdom’s Science and Technology Facilities Council, the Chilean Comisión Nacional de Investigación Científica y Tecnológica (CONICYT), and the National Research Foundation of Korea. The Southeastern Universities Research Association (SURA) operated the Thomas Jefferson National Accelerator Facility for the US Department of Energy under Contract No.DE-AC05-84ER40150.

-
- [1] The phenomenology of color flux-tubes which can “break” through the creation of $q\bar{q}$ pairs has a long history. Extending Schwinger’s calculation, J. Schwinger, Phys. Rev. **82**, 664 (1951), of the vacuum production of e^+e^- pairs in an external electric field, the pioneering papers of L. Micu, Nucl. Phys. **B10**, 521 (1969), and of R. Carlitz, M. Kislinger, Phys. Rev. **D2**, 336 (1970) introduced the concept of $q\bar{q}$ vacuum pair creation. The binding force was approximated as a harmonic oscillator potential by A. LeYaouanc *et al.*, Phys. Rev. **D8**, 2223 (1973). In 1979 A. Casher, H. Neuberger, S. Nussinov, Phys. Rev. **D20**, 179 (1979) proposed a shorthand heuristic for describing the color flow between quarks, and Neuberger added finite time corrections in H. Neuberger, Phys. Rev. **D20**, 2936 (1979).
- [2] B. Andersson’s review, “The Lund Model,” Cambridge Univ. Press, 1998, as a modern overview.
- [3] See results from the **UA1**, C. Bocquet *et al.*, Phys. Lett. **B366**, 447 (1996), **Jade**, W. Bartel *et al.*, Z. Phys. **C20**, 187 (1983) and **Tasso** collaborations, M. Althoff *et al.*, Z. Phys. **C27**, 27 (1985). For a summary of earlier measurements of the strangeness suppression factor, see A. Wroblewski, Acta Phys. Pol. **B16**, 379 (1985); P.K. Malhotra, R. Orava, Z. Phys. **C17** (1983) 84, and references therein.
- [4] See <http://home.thep.lu.se/~torbjorn/Pythia.html> for general information on the “LUND-Model” family of event generators.
- [5] Results from the **OPAL**, G. Alexander *et al.*, Phys. Lett. **B264**, 467 (1991), and **SLD** Collaborations, K. Abe *et al.*, Phys. Rev. **D59**, 052001 (1999).
- [6] Results from the **H1** Collaboration, F.D. Aaron *et al.*, Eur. Phys. J. **C61** (2009) 185.
- [7] P. Ambrozewicz *et al.*, Phys. Rev. **C75**, 045203 (2007).
- [8] B.A. Mecking *et al.*, Nucl. Inst. Meth. **A503**, 513 (2003).
- [9] See, e.g., Eq. (5-11) in “Elementary Particles” by William R. Frazer, Prentice-Hall, (1966).
- [10] K. Park, M.D. Mestayer, CLAS Analysis Note 2013-103.
- [11] The bin sizes and virtual photon flux-factors are the same for the three channels and thus divide out in the ratio.
- [12] M.M. Kaskulov, K. Gallmeister, U. Mosel, Phys. Rev. **D78**, 114022 (2008).
- [13] E.A. Hawker *et al.*, Phys. Rev. Lett. **80**, 3715 (1998).
- [14] K. Ackerstaff *et al.*, Phys. Rev. Lett. **81**, 5519 (1998).